



Structural, DC Conductivity and Dielectric Characteristics of PVA/CMC/PPy/Melanin Blended Polymer Composites for Energy Storage Applications

A. M. El-naggar¹ · Lamya A. Alsulaymani² · Mohamed Bakr Mohamed³ · A. M. Kamal² · A. A. Albassam¹ · A. M. Aldhafiri²

Received: 15 May 2024 / Accepted: 6 June 2024

© The Author(s), under exclusive licence to Springer Science+Business Media, LLC, part of Springer Nature 2024

Abstract

The objective of this study is to produce polyvinyl alcohol (PVA)/carboxymethyl cellulose (CMC)/polypyrrole (PPy)/ x wt% melanin blended polymers as future materials to utilize in the promising applications of electronic and storage energy fields. The structures and morphologies of the blends were investigated using X-ray diffraction and scanning electron microscopy techniques. The dielectric constant increased at 100 kHz from 55 to 8.6×10^4 as the host blend doped with 0.25 wt% melanin. The values of the energy density (U) were increased as the amount of melanin doping excess $x=0.1$ wt% and it has the maximum value 5.41 J/m^3 as $x=0.25$ wt% at 100 Hz. The values of U for all blends increased as the temperature rose. Blend with $x=0.25$ wt% has the highest ac conductivity. The conduction mechanisms in different blends were identified through the application of different theoretical models. The influence of the amount of melanin doping and temperatures on the real and imaginary parts of the electric impedance and the electric modulus, as well as the Nyquist curves was studied. Blend with $x=0.2$ wt% has the highest dc conductivity ($3.74 \times 10^{-8} \text{ S m}^{-1}$). All blends exhibit one or two activation energy values based on the temperature range and the amount of dopant. In conclusion, the outcomes obtained from the experiment demonstrated that the blended polymers consisting of PVA/CMC/PPy/ x wt% melanin possess exceptional electrical properties, rendering them potentially valuable in the fields of energy storage and electronics.

Keywords PVA/CMC/PPy/melanin · Conduction mechanisms · AC conductivity · Activation energy

1 Introduction

Lighter and more efficient devices are made possible by polymers, which are essential for developments in the energy, communication, and electronics industries [1]. Polyvinyl alcohol (PVA) is a water-soluble polymer that has a semi-crystalline structure. It is non-toxic, biocompatible, and environmentally friendly. PVA has good film and fiber

forming abilities, as well as good mechanical characteristics. It also exhibits remarkable resistance to chemicals and is biodegradable [2]. Carboxymethyl cellulose (CMC) is a chemically altered natural polymer that has a remarkable ability to absorb water. CMC is biologically harmless and can be used safely with mucous membranes, bones, and skin. CMC can serve as a substrate for wound healing and the regeneration of skin [3]. One benefit of CMC is its capacity to blend with other polymers, such as PVA, which possesses biocompatibility, lower toxicity, and hydrophilicity [4].

Polypyrrole (PPy) is a highly researched polymer because it is environmentally stable, relatively easy to synthesize, and has good electrical conductivity. The PPy is widely utilized in various commercial applications, including batteries, super capacitors, sensors, and corrosion protection [5]. Melanin is a cost-effective and naturally-occurring substance that possesses biodegradable and biocompatible properties [6].

✉ Mohamed Bakr Mohamed
mbm1977@yahoo.com

¹ Research Chair of Exploitation of Renewable Energy Applications in Saudi Arabia, Physics & Astronomy Department, College of Science, King Saud University, P.O. Box 2455, 11451 Riyadh, Saudi Arabia

² Physics & Astronomy Department, College of Science, King Saud University, P.O. Box 2455, 11451 Riyadh, Saudi Arabia

³ Physics Department, Faculty of Science, Ain Shams University, Cairo, Egypt

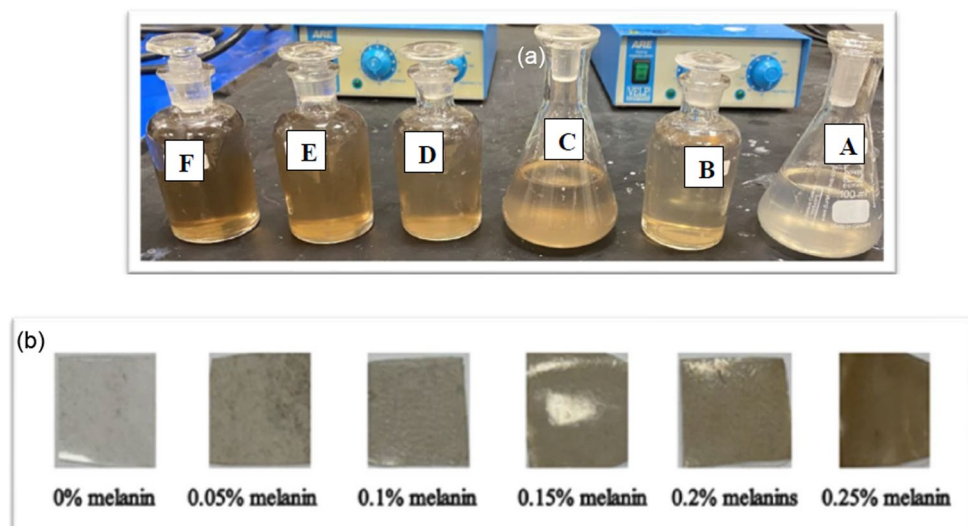
A defining feature of a polymer or blended polymer is the inclusion of fillers that are evenly distributed throughout the polymer matrix. Polymer composite, or blends of polymers with fillers, exhibit better features in comparison to conventional polymers, making them suitable for use in different applications. For instance, increasing of SiO₂NPs in high viscosity carboxymethyl cellulose HVCMC, poly (N-vinyl pyrrolidone) PVP and polyethylene glycol PEG polymer blend from 0% to 0.045% leads to rise in the values of the attenuation coefficient [7]. The dielectric constant (imaginary, real) was enlarged with the raised amount of strontium oxide NPs doped amount in PVA-PEG blend [8]. Lin et al. prepared a dual-physical crosslinking (DP) carboxymethyl cellulose (CMC) hydrogel with high-toughness, healability, and electric conductivity by integrating abundant ions into the matrix [9]. The dielectric and energy dissipation features of polyvinyl alcohol (PVA) and Dextrin have been significantly enhanced by the utilise of SiO₂NPs. Additionally, the sensitivity to relative humidity has been demonstrated in a variety of NPs ratios, temperatures, times and RH ranges [10]. The optical and carbon dioxide gas sensing features of polythiophene were enhanced by dispersion of manganese dioxide nanoparticles [11].

Mirmahalleh et al. produced cellulose/polypyrrole composites to be included in polymer electrolytes for use in lithium-ion batteries [12]. According to Pan et al. polymer composites with a high dielectric constant, low loss, and high breakdown can be made using sandwich-structured PPy/MoS₂/PPy nanosheets [13]. An in situ hybrid polymerization process was used to improve the specific capacitance of a cotton fibre electrode with PPy and MXene [14]. At higher temperatures, the dielectric properties of the PVDF/PPy blend improved so it can be

used in electromagnetic wave shielding and high temperature sensing [15]. The PY-C/PVA/LiO nano-composite shows great potential for use in the production of nano-electronic devices [16]. Higher levels of melanin doped PVP/CMC blend were associated with a rise in dielectric constant, dielectric loss, and AC conductivity, all of which reduced as the melanin content approached 0.5 wt% [6]. The environmentally friendly PVA/PPy polymeric material has applications in biosensors, capacitors, Electromagnetic Interference (EMI)/Radio Frequency Interference (RFI) shielding, and insulation [17]. The hydrogel electrodes, called “Mela Gel”, were formed using cellulose nanofibrils (CNFs), melanin, and PPy. The Mela Gel electrodes exhibited exceptional conductivity and energy storage capacity, with an impressive energy density of 5387 mWh/kg. This makes them particularly suited for specific sensors [18]. For environmentally friendly electronics, Nozella et al. created an organic mixed ionic electronic conductor (OMIEC) using a blend of melanin and poly(3,4-ethylenedioxythiophene) polystyrene sulfonate (PEDOT:PSS) [19]. Agrawal et al. fabricated 3D fibrous scaffolds using melanin-poly (3-Hydroxybutyrate) for the purpose of neural tissue engineering [20]. Using PPy embedded in a PVA matrix, Das et al. created an ethanol sensor that works at room temperature [21]. The dielectric constant, dielectric loss, and AC conductivity of polyvinyl pyrrolidone/carboxymethyl cellulose/ melanin were reduced first as the quantity of melanin reached 0.5 wt% then rose again with further raises in melanin amounts. The Nyquist plot is affected by the quantity of melanin doping. Undoped blends are less capacitive than doped blends, particularly those that have 0.5 wt% melanin [6].

The present study aimed to produce polymer blends employing the casting technique, comprising of PVA/CMC/PPy/x wt%

Fig. 1 The **a** the solutions and **b** films for PVA/CMC/PPy/x wt% Melanin blended polymers



melanin. The impact of the doping concentration of melanin on the structure and morphology of the produced blends was investigated. The current study also attempted to examine the impact of melanin doping, frequency, and temperature on the dielectric constants, ac conductivity, impedance, electric modulus, and activation energy of the PVA/CMC blended polymer.

2 Methods and Materials

2.1 Materials Preparation

The polymer blends consisting of PVA/CMC/0.1 wt%PPy/x wt% melanin ($x=0, 0.05, 0.1, 0.15, 0.2, 0.25$) were created using the casting method, Fig. 1. In this process, polyvinyl alcohol (PVA, MW = 50,000 g/mol, Acros organics, 98%), carboxymethyl cellulose (CMC, in the form of sodium carboxymethyl cellulose, MW = 90,000g/mol, Sigma Aldrich, 99%), polypyrrole (PPy, conductivity 10–50 S/cm, Sigma Aldrich, 99.5%), and melanin sourced from natural low-cost *Nigella sativa* melanin extracted within the pilot plant labs at King Saud University (KSU) [6] were used. The process was carried out as follows: (i) x wt% melanin were dissolved in 15 ml deionized distilled water at room temperature (RT) for 24 h utilizing a magnetic stirrer until clear solutions were achieved. (ii) 1 g of PVA was dissolved in 65 ml dimethyl sulfoxide (DMSO, VWR chemicals) at 50 °C for 0.5 h via a magnetic stirrer until a clear solution was established then let cool to RT . (iii) 1 g of CMC was added to the melanin solutions and let to dissolve at RT utilizing a magnetic stirrer to develop clear solutions. (iv) 0.1% PPy was added to the (CMC + melanin) solutions and allowed to distribute for 0.5 h by a magnetic stirrer. (v) The above solution (CMC + melanin + PPy) was mixed with PVA solution at 50 °C for 1 h with a magnet stirrer then placed in ultrasonic bath at 50 °C for 3 h, then put on a magnetic stirrer at 50 °C for 24 h until clear solutions were achieved. (vi) The resultant solutions were poured into Petri dishes and put in an electric furnace at 70 °C for 5–6 days. (vii) PVA/CMC/PPy/melanin blends were established with a thickness of 0.20–0.36 mm (measured by a digital micro-meter).

$$x(\text{wt}\%) = \frac{W_{\text{PPy}}}{W_{\text{PVA}} + W_{\text{CMC}} + W_{\text{PPy}} + W_{\text{melanin}}} \times 100 \quad (1)$$

where W_{PVA} , W_{CMC} , W_{PPy} and W_{melanin} are the weights of PVA, CMC, PPy and melanin respectively.

2.2 Materials Characterizations

The structural investigations of all blends and filler samples were done utilising a PANalytical X-ray diffractometer (X'pert MPD model copper source). Images from a scanning electron microscope (SEM) were acquired using the JED-2200 Series from JEOL, Akishima, Tokyo, Japan.

The dielectric constant parameters at different temperatures were determined by applying a 2 V ac voltage and measuring the variations in capacitance (C_p) and dissipation factor (D) using a GwINSTEK LCR 8105G device (INSTEK AMERICA Corp., USA) instrument.

The subsequent formulas [1] were used to calculate the values of the dielectric constant (ϵ' , ϵ''), ac conductivity (σ_{ac}), complex electric modulus ($M^* = M' + iM''$), and energy density (U):

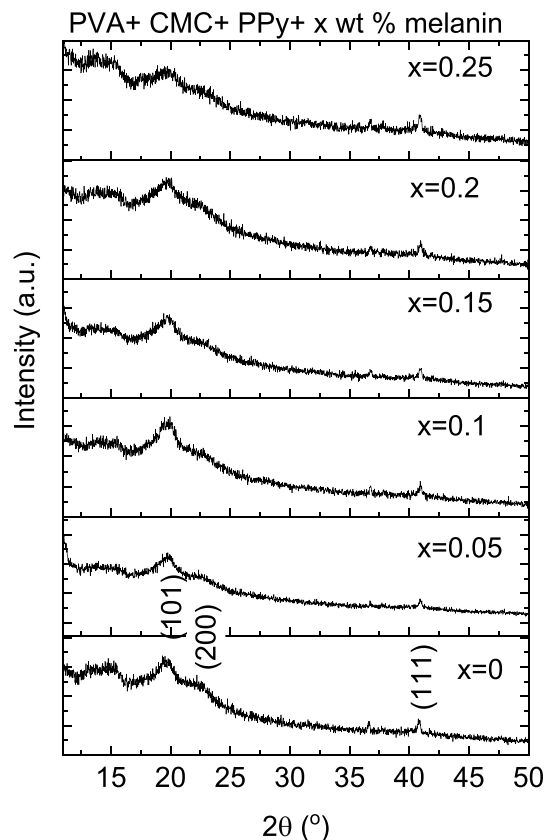


Fig. 2 XRD data for PVA/CMC/PPy/x wt% Melanin blended polymers

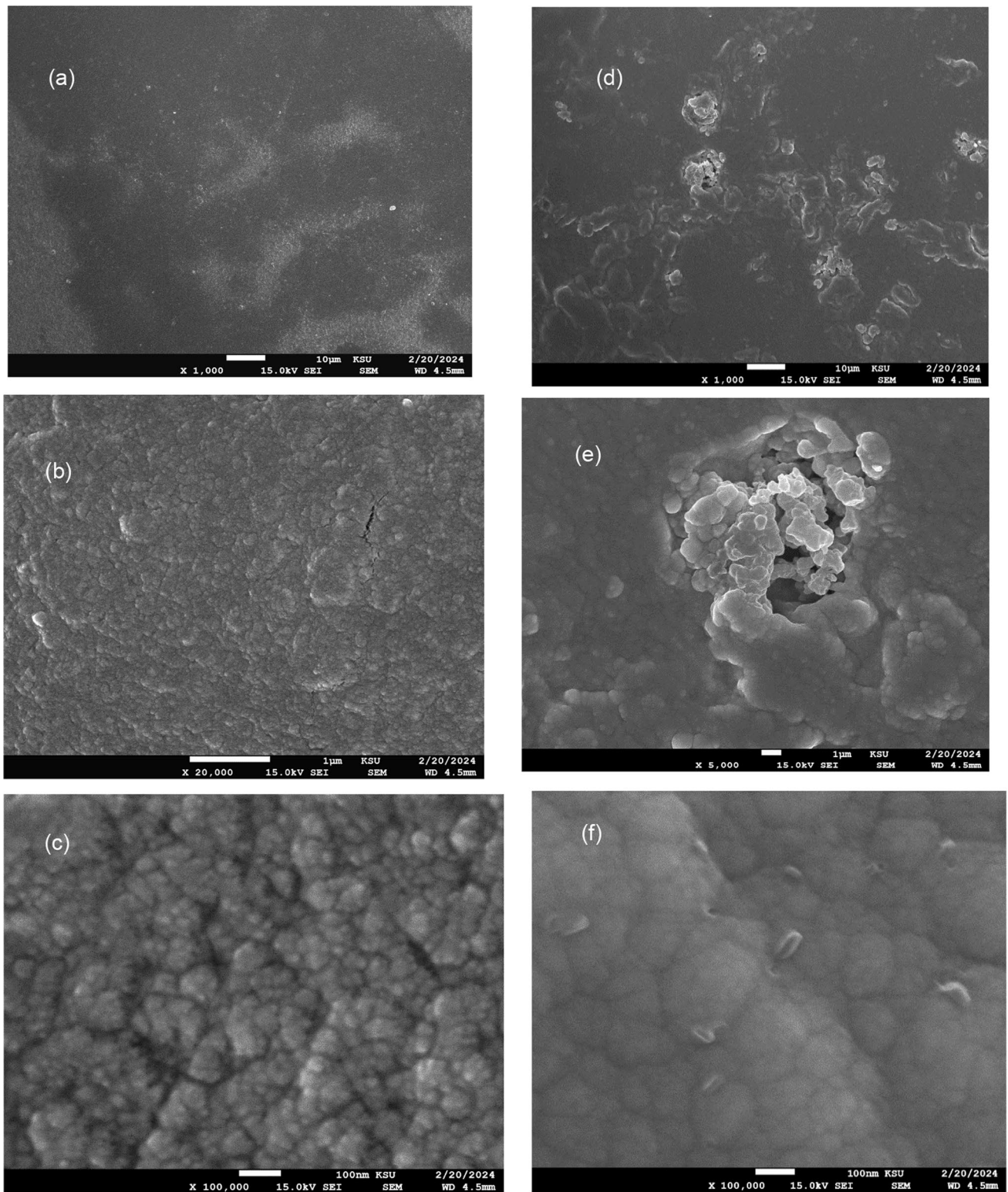


Fig. 3 SEM images for PVA/CMC/PPy/x wt% Melanin blended polymers with **a–c** $x=0$ and **d–f** $x=0.2$

$$\epsilon' = \frac{Cd}{\epsilon_0 A} \quad (2)$$

$$a\sigma_{ac} = 2\pi f \epsilon_0 \epsilon' \tan \delta \quad (3)$$

$$\tan \delta = \epsilon'' / \epsilon' \quad (4)$$

$$M' = \frac{\epsilon'}{\epsilon'^2 + \epsilon''^2} \quad (5)$$

$$M'' = \frac{\epsilon''}{\epsilon'^2 + \epsilon''^2} \quad (6)$$

$$U = \frac{1}{2} \epsilon_0 \epsilon_r E^2 \quad (7)$$

where ϵ_0 and A are the permittivity of free space and area of the disc, respectively. A system that was used to measure electrical conductivity involved a motor pump for cooling with liquid nitrogen and a Janis VPF-100 cryostat. Keithley 6517-BA, an electrometer, was used to measure the current. The values of conductivity were measured by two points measurement.

3 Results and Discussion

3.1 Structural Analysis

Figure 2 demonstrates the X-ray diffraction (XRD) patterns of polymers blended with PVA/CMC/PPy/x wt% melanin. All the peaks observed in Fig. 2c can be ascribed to the PVA/CMC blend, whereas none of the peaks corresponding to the PPy or melanin fillers could be identified due to its remarkable compatibility with the PVA/CMC matrix. The main diffraction peak observed at 19.9° in the PVA/CMC blend indicates its semicrystalline characteristic, as the blend comprises the semi-crystalline polymer PVA [22]. This peak confirmed the existence of CMC and PVA polymers [22, 23]. The peaks at 19.9° , 22.6° and 40.8° belong to the (101), (200) and (111) crystal planes of PVA [22]. This suggests that there are substantial interactions taking place among the constituents of the blend. Furthermore, melanin alters the configuration of the mixture's crystals and modifies the non-crystalline regions. Then, this influences the mobility of segments,

which impacts ion transport and, ultimately, electrical conductivity.

To evaluate the impact of doping on the blend's morphology, scanning electron microscopy (SEM) images were used to examine the surface morphologies. Figure 3 presents the results obtained from examining the undoped and doped blends containing 0.2 wt% melanin at various magnifications. The undoped blend images exhibit a homogeneous and rough surface devoid of any cracks. Significantly,

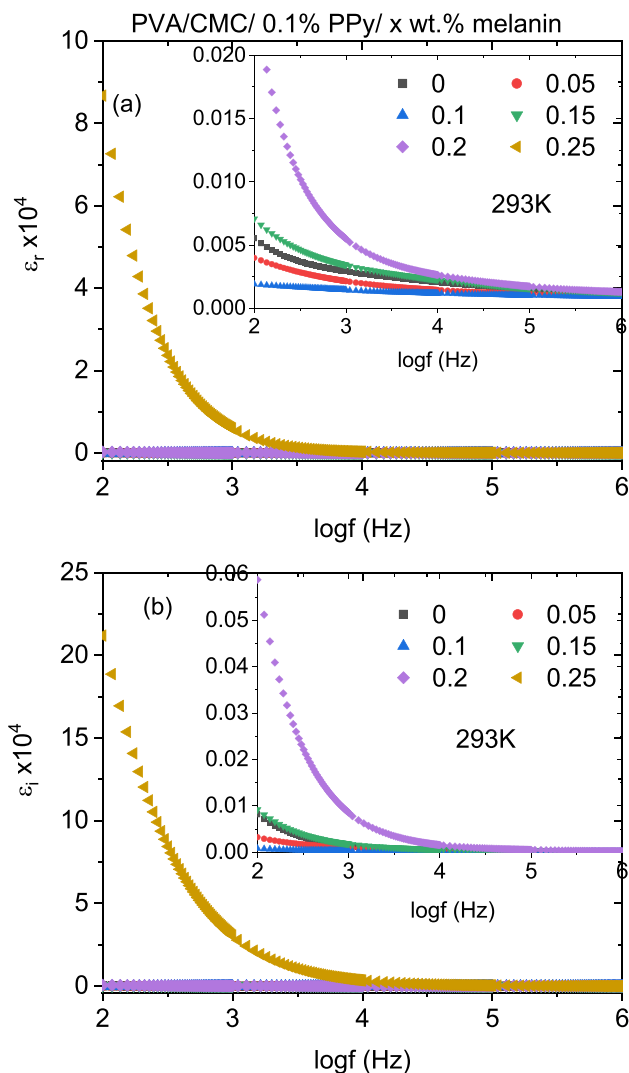


Fig. 4 Variation of **a** real and **b** imaginary parts of the dielectric constant with frequency for PVA/CMC/PPy/x wt% Melanin blended polymers

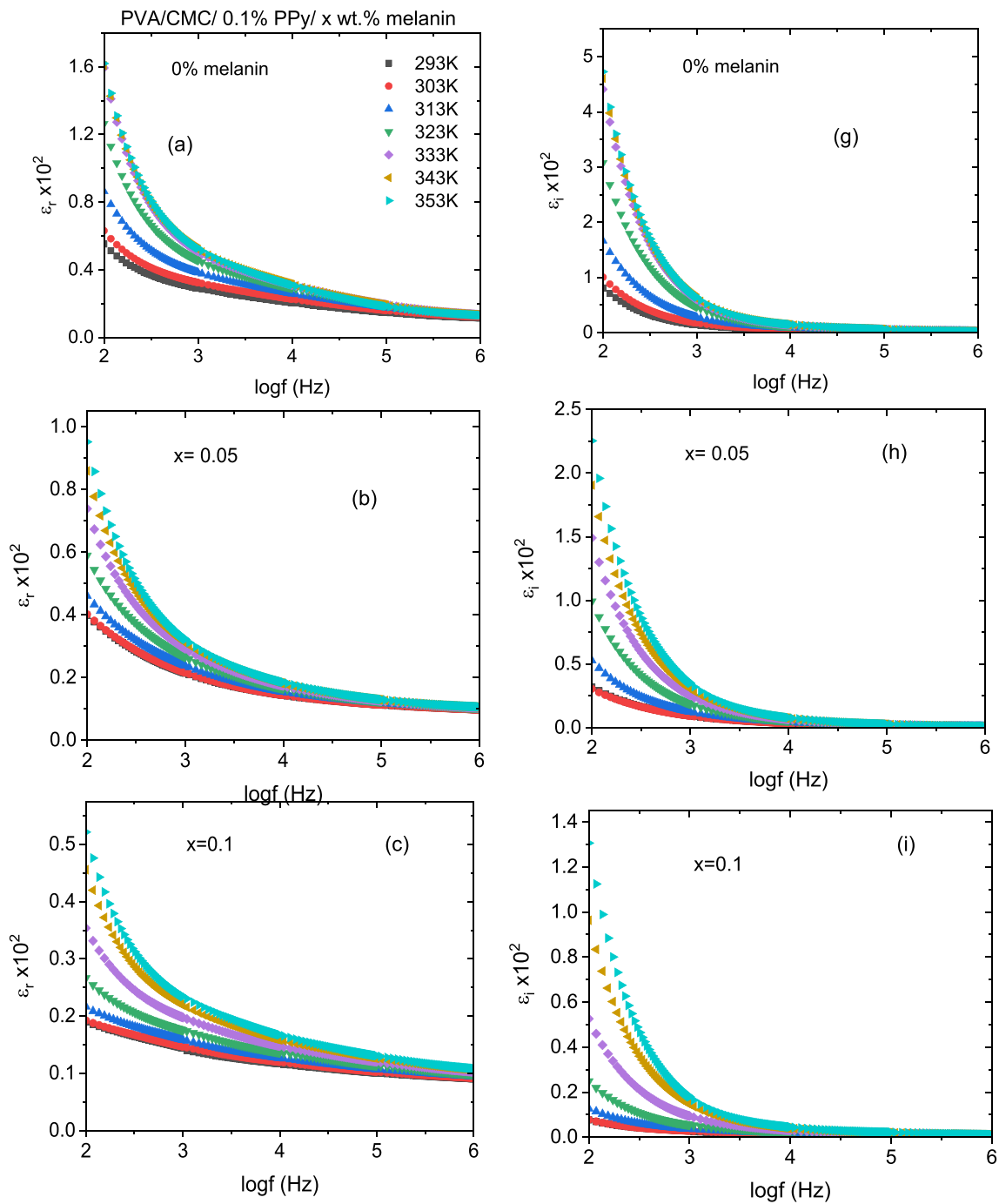


Fig. 5 Variation of **a–f** real and **g–i** imaginary parts of the dielectric constant with frequency for PVA/CMC/PPy/x wt% Melanin blended polymers at different temperatures

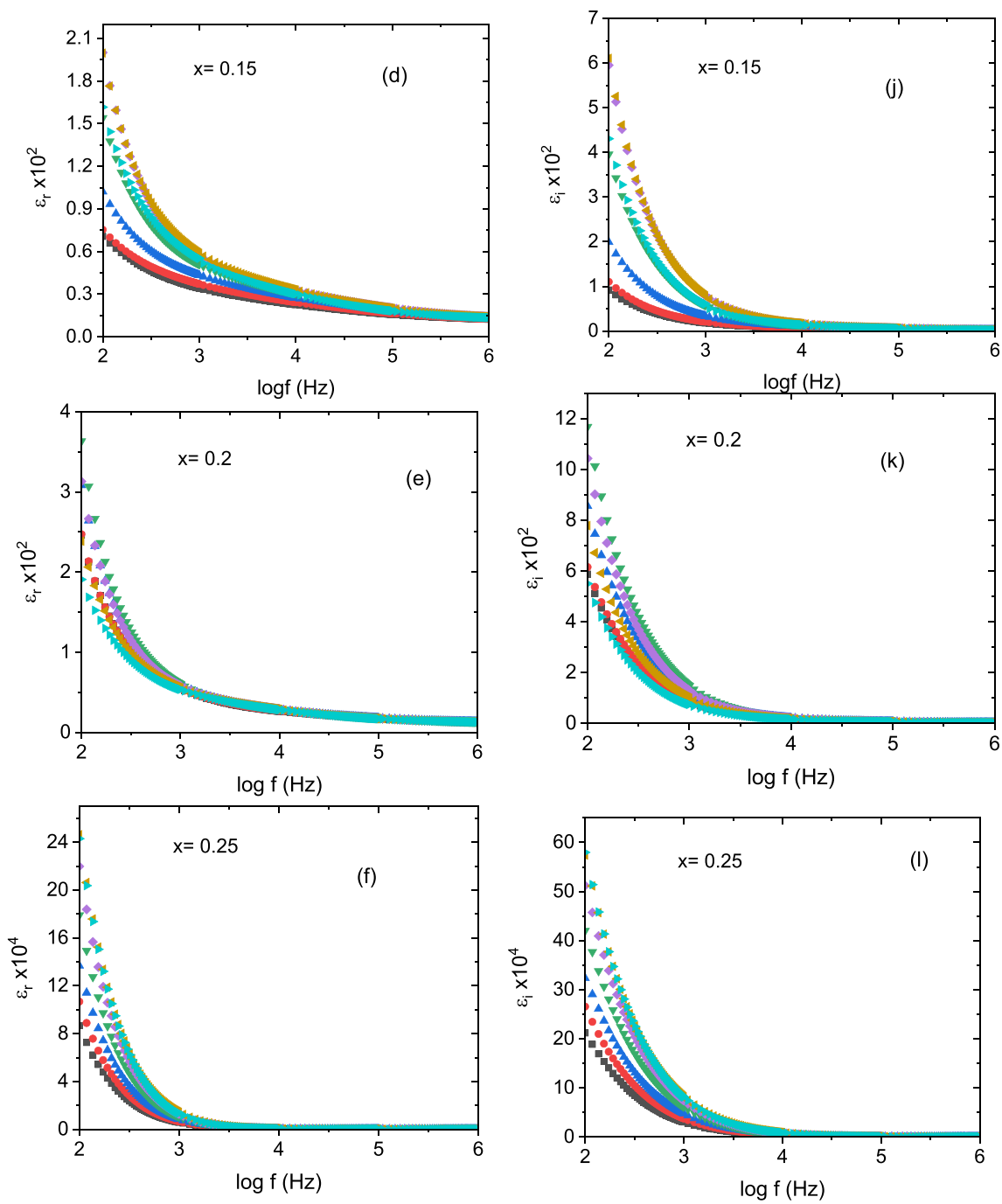


Fig. 5 (continued)

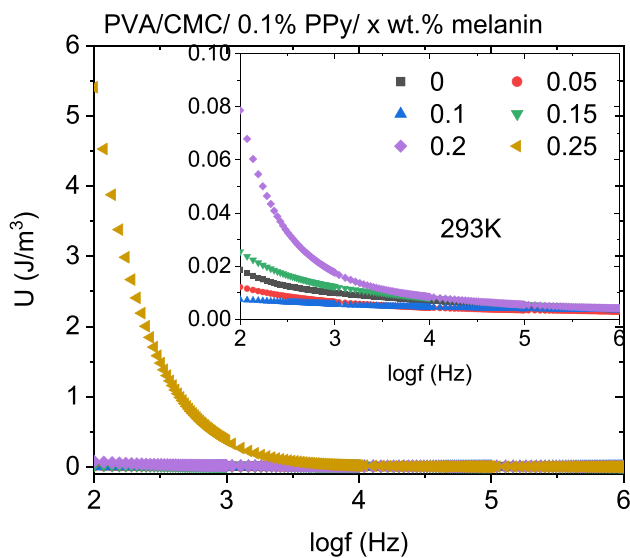


Fig. 6 Variation of energy density with frequency for PVA/CMC/PPy/x wt% Melanin blended polymers at 293 K

the abundance of numerous chunks or aggregates on the upper surface of the polymer composite films suggests that melanin has a tendency to accumulate and disperse within the polymer matrix. Consequently, the blend that has been doped with melanin exhibits an increased level of roughness.

3.2 AC Conductivity Analysis

The particular features of materials in terms of their ability to polarize at specific frequencies are of significant importance. In systems consisting of multiple components, the movement of mobile charge carriers across the materials causes the accumulation of space charges at the interfaces between these components, resulting in differences in dielectric constants and conductivity. Interfacial polarization is a phenomenon that greatly affects permittivity changes with frequency, especially at lower frequencies because of the complex movements of chain segments that resemble micro-Brownian motion [24]. Figure 4a illustrates the frequency dependence of the real part of the dielectric constant (ϵ') of PVA/CMC/PPy/x wt% melanin blended polymers at 293 K. The graph demonstrates that the ϵ' values of all the doped and undoped blends have a similar frequency dependence. PVA/CMC/PPy/x wt%

melanin blended polymer exhibits a low-frequency dispersion characterized by a change in the frequency of ϵ' , indicating the presence of significant dispersion at low frequencies. Dispersion at low-frequency in PVA/CMC/PPy/x wt% melanin blended polymers is observed, as indicated by the frequency variation of ϵ' . The low-frequency dielectric features of these blends are influenced by many factors, including AC conductivity, bipolar orientation, charge transporters, and electrode computing. Interfacial, dipolar, and ionic polarization lose their effectiveness at higher frequencies, leaving only the AC electrical conductivity parameter to be important. The decrease in ϵ' as frequency increases can be attributed to the shorter time available for the interfacial bipolar to align themselves in response to the field [25]. As the percentage of melanin rose up to 0.1 wt%, the dielectric properties of the doped blend initially decreased, but subsequently rose again with further melanin doping. The increase in ϵ' values can be attributed to the accumulation of charge carriers and an elevation in polarization. On the other hand, the reduction in ϵ' values may be ascribed to the clustering of melanin at the boundaries between particles, leading to the formation of structural defects. The existence of these imperfections resulted in the accumulation of electrically charged particles at the boundaries, causing a decrease in the movement ability of the particles and the arrangement of electric dipoles when an external force was applied. Thus, the polarization decreased [26]. Figure 4b depicts the correlation between the variation of ϵ'' and frequency for all blends. The values of ϵ'' demonstrate a comparable pattern to that of ϵ' . The rise in the values of ϵ'' at lower frequencies can be caused by conduction losses [25]. At high frequencies, the drop in ϵ'' can be attributed to the heat generated within the composite material as a result of the rapid reorientation of dipoles in response to the rapidly changing direction of the electric field [27]. According to Fig. 5, the dielectric constants of all the blends consistently increase as the temperature rises. The rise in dielectric permittivity with temperature can be attributed to the acceleration of charge carrier alignment due to thermal energy, as well as the rapid alignment of dipoles [28]. Similar results were detected in as-synthesized polythio-phen (PTh) [29]. The inclusion of PPy and varying concentrations of melanin in doped blends influences the orientation of the electric dipoles in the host blends (PVA/CMC), consequently impacting the values of the dielectric constants. Figure 6 illustrates the

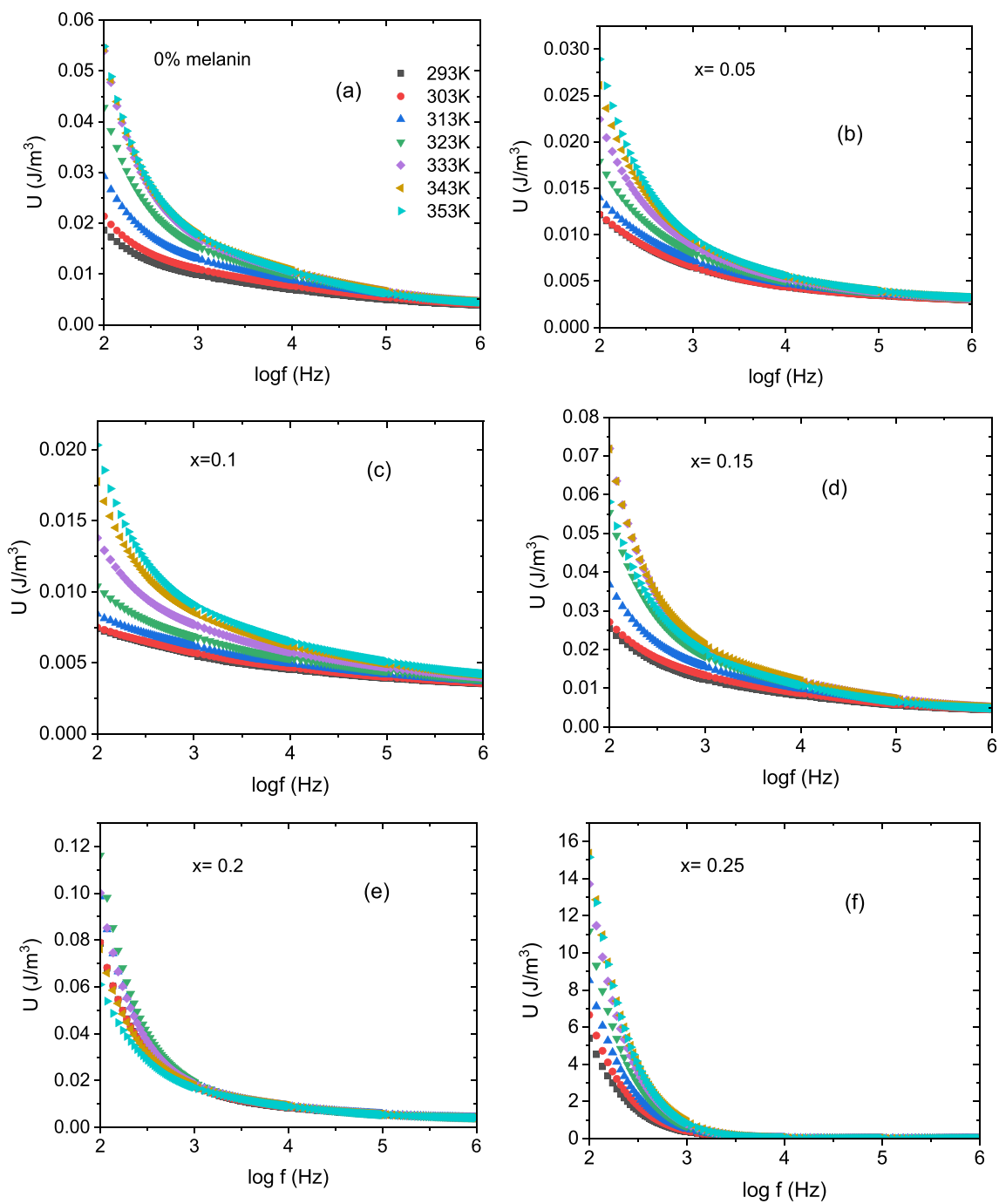


Fig. 7 a–f Variation of energy density with frequency for PVA/CMC/PPy/ x wt% Melanin blended polymers at different temperatures

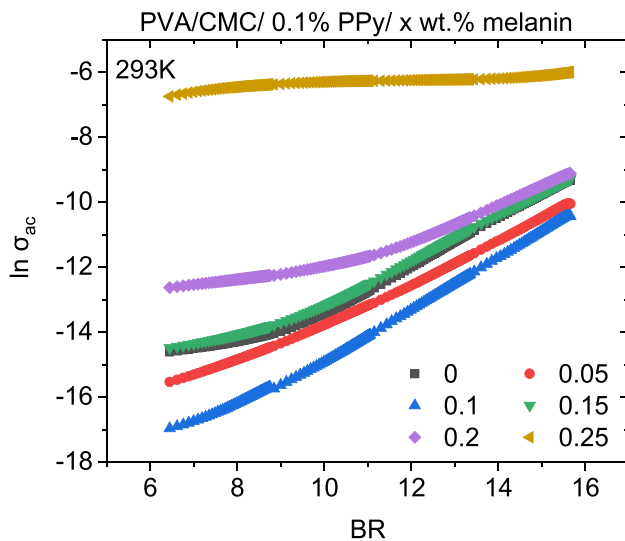


Fig. 8 Frequency dependence of the ac electrical conductivity for PVA/CMC/PPy/x wt% Melanin blended polymers at 293 K

relationship between frequency and energy density (U) in PVA/CMC/PPy/x wt% melanin blended polymers at a temperature of 293 K. The plot illustrates that the U values initially declined with increasing amounts of doped melanin up to $x=0.1$ wt%, after which they began to rise again as the melanin doping quantity rose further. Figure 7 shows that the values of U for all blends increased as the temperature rose. However, for the doped blend with $x=0.2$ wt% melanin, the U values varied irregularly as the temperature increased. These outcomes validate the utilization of a majority of PVA/CMC/PPy/x wt% melanin blended polymers as suitable materials for energy storage.

One crucial physical characteristic that makes polymeric materials useful in electrical applications such as contact switches and transistors is their AC conductivity (σ_{ac}). Figure 8 depicts the correlation between the variation in the σ_{ac} and the frequency for PVA/CMC/PPy/x wt% melanin blended polymers at 293 K. It is evident that the σ_{ac} increased as the frequency increased in all blends. Improved electronic interaction mechanisms happening within the materials, which result in greater conductivity, might be responsible for this behavior. Furthermore, as the frequency of the applied electric field increases, the interactions between fillers and the surrounding matrix in

blended polymers may lead to enhanced charge transfer pathways, which encourages higher electrical conductivity. The σ_{ac} initially dropped when PVA/CMC/PPy was doped with melanin up to a concentration of 0.1 wt%. However, it gradually rose as the quantity of melanin was further raised. The modifications seen were dependent on the degree of melanin dispersion within the host blend matrix. Consequently, the degree of interaction between the filler and host blend was modified. This interaction results in the creation of a remarkably effective pathway for the conduction of electricity within the polymer matrix. The increase in conductivity can be related to the modification in the non-crystalline properties of the blended polymer, which affects the energy barrier and subsequently improves the motion of ions. One explanation for the decline in σ_{ac} values is the aggregation of melanin. Where the conductivity drops when ion aggregation reduces the number of mobile charge carriers [30]. Figure 9 shows the relationship between frequency and the change in $\ln \sigma_{ac}$ at different temperatures for polymers blended with various melanin contents. Like many polymers and semiconductors, it seems that the σ_{ac} improves with rising temperatures [31]. As temperatures are elevated, the number of transit sites increases and the movement of charge carriers in the blends is improved [32]. More charge carriers are able to pass the potential barrier and contribute to electrical conduction because this makes moving between transit sites easier with minimal energy gain.

The electrical conduction in different blends are governed by Jonscher's power law [33].

$$\sigma_{ac}(\omega) = \sigma_0 + B\omega^s \quad (8)$$

where σ_0 , $\omega = 2\pi f$, $B(T)$ and $0 \leq s(T) \leq 1$ are the dc conductivity, angular frequency, constant and frequency exponent, respectively.

The conduction mechanism of AC conductivity can be identified through the application of different theoretical models, including quantum mechanical tunnelling (QMT), correlated barrier hopping (CBH), non-overlapping small polaron tunnelling (SPT), and overlapping large polaron tunnelling (OLPT) [33]. According to the QMT model, which is based on phonon-assisted electron tunnelling, the value of s will either increase slightly with temperature or stay the same. The CBH model proposes

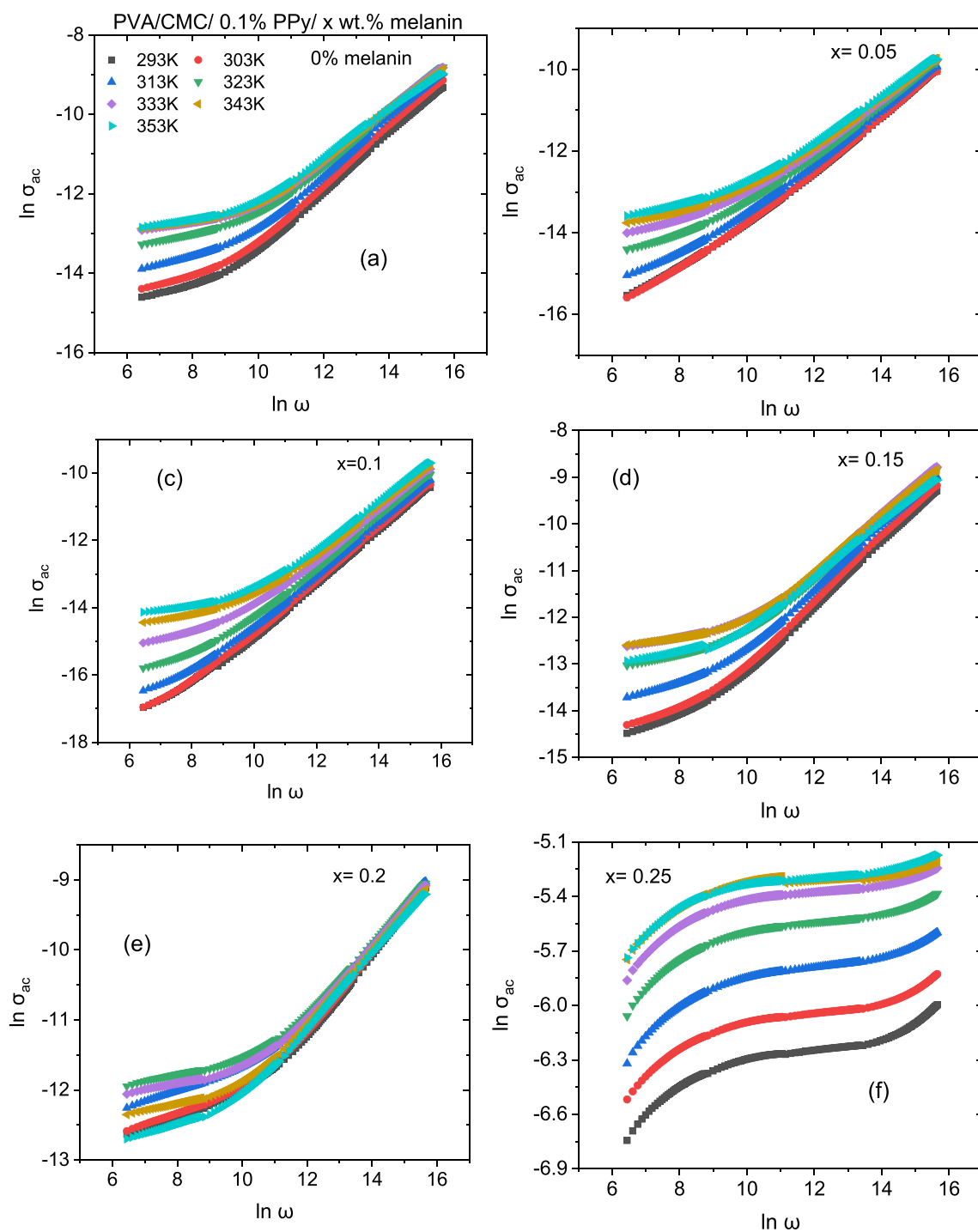


Fig. 9 a–f Frequency dependence of the ac electrical conductivity for PVA/CMC/PPy/x wt% Melanin blended polymers at different temperatures

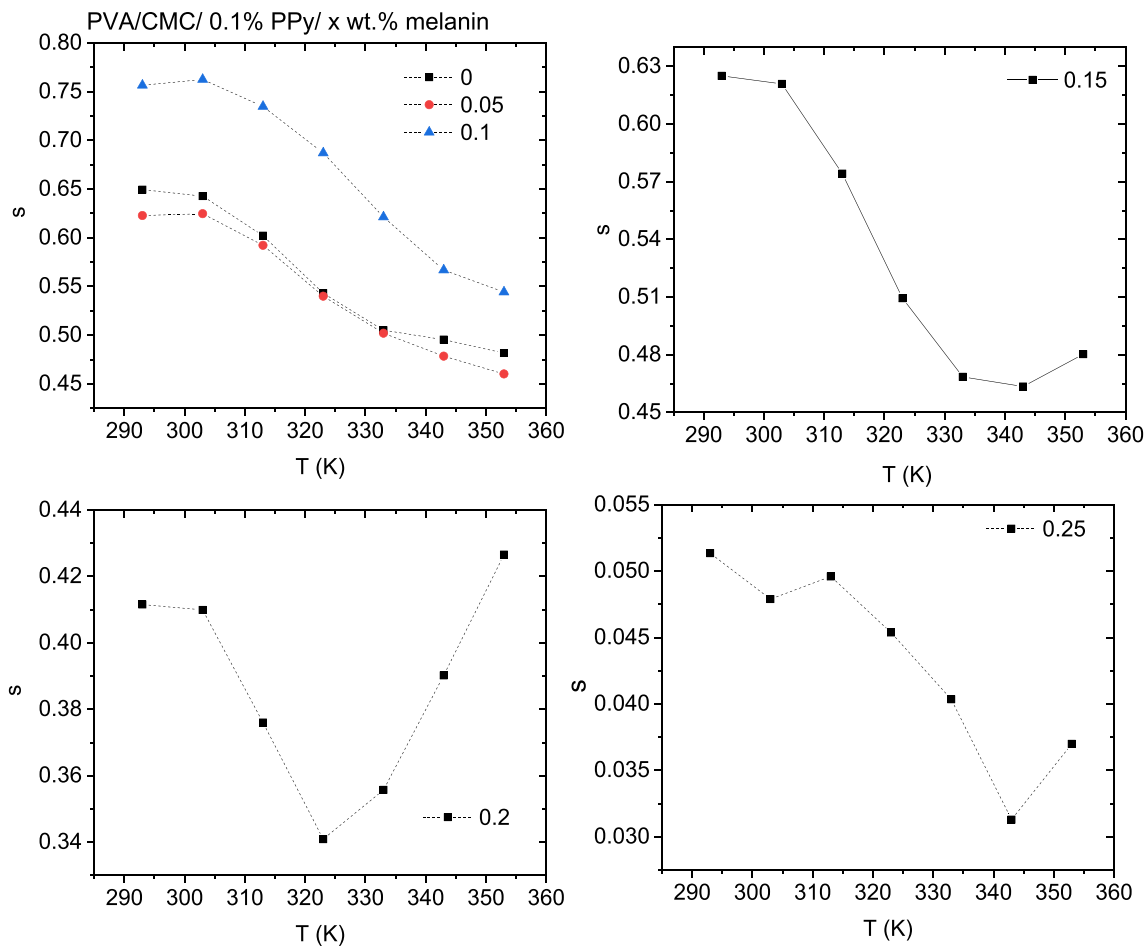


Fig. 10 Variation of s parameter with temperature for PVA/CMC/PPy/ x wt.% Melanin blended polymers

that the charge carriers engage in hopping between two sites positioned above the Coulomb barrier, which serves as an obstacle separating them. Furthermore, the model indicates that the exponent s diminishes with increasing temperature. According to the SPT model, the value of s will consistently increase as the temperature rises. On the other hand, the OLPT model suggests that s will initially decrease with temperature until a certain point, after which it will start to increase again with further temperature rise.

Utilizing the subsequent relationship, we can create a relationship plot between $\ln\sigma$ and $\ln\omega$ at various temperatures (Fig. 9) to find different values of s in our case:

$$\ln\sigma = \ln B + s \ln(\omega) \quad (9)$$

As the temperature grew, the s values for undoped and doped blends containing x up to 0.1 wt% dropped, Fig. 10. As a result, these blends followed the CBH model. Conversely, as the temperature rose, the s values in the other blends rose once more after first decreasing to a particular

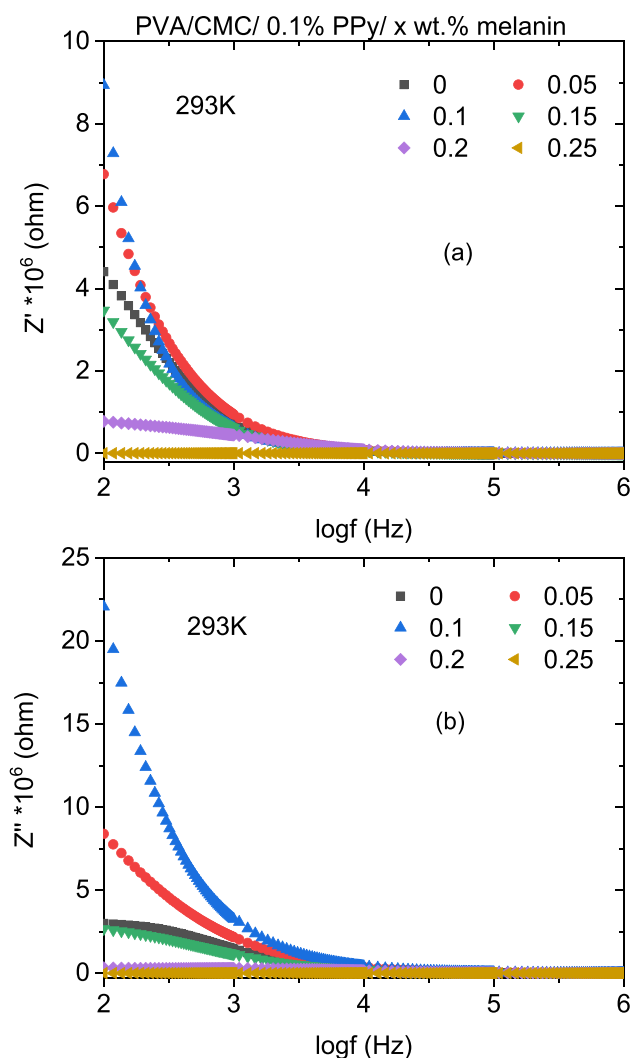


Fig. 11 Frequency dependence of the **a** real and **b** imaginary parts of complex impedance for PVA/CMC/PPy/ x wt% Melanin blended polymers at 293 K

point. These suggest that the OLPT model is followed by these blends.

Impedance spectroscopy is a widely used and effective technique for studying the electrical properties of electrolytes and their interaction with electrically conductive electrodes. Both the electrode polarization and the kind of charge carriers (electrons or ions) can be inferred from

an analysis of the impedance spectrum structure. The impedance of PVA/CMC/PPy/ x wt% melanin blended polymers at 293 K is represented by the real component (Z') and the imaginary component (Z'') as a function of frequency. These components are illustrated in Figs. 11a and b, respectively.

The plot illustrates a decrease in the real component of impedance for all samples as the frequency increases, indicating an increase in the AC conductivity within the extended frequency range. The combination of the real part of the impedance at higher frequencies for all blends indicates that the blended polymers release space charge, which lowers the barrier potential. The accumulation of space charge polarization impact in all blends is indicated by the merging of Z'' values at higher frequencies [34]. The Z' and Z'' values of PVA/CMC/PPy/ x wt% melanin were grown by melanin doping up to $x = 0.1$ then declined with increase the quantity of melanin further.

Figure 12 depicts the changes in Z' and Z'' of the electrical impedance at various frequencies and temperatures for PVA/CMC/PPy/ x wt% melanin blends. As the temperature and frequency increase, the values of Z' gradually decrease, indicating an improvement in the σ_{ac} values [35]. This behavior implies that when the material is exposed to high temperatures and low frequencies, the space charge polarization effect builds up [36, 37]. In contrast, the values of Z' tend to decrease towards zero as the frequency increases and are not influenced by temperature. This could be attributed to the discharge of space charge at higher temperatures [38]. The Z'' spectra display a comparable pattern to Z' , except for blends with an x value of up to 0.15 wt%. Blends with $x = 0.15$ and 0.2 wt% showed identifiable and wide peak while blend with $x = 0.25$, it has two peaks with noticeable asymmetry. As the temperature rises, the Z'' peak maximum undergoes a shift in relation to the frequency, and the temperature also affects the height of these peaks. According to these findings, the relaxation time varies amongst the samples [36].

Figure 13 depicts the Nyquist curves that demonstrate the correlation between Z' and Z'' of PVA/CMC/PPy/ x wt% melanin blended polymers at a temperature of 293 K. The Cole–Cole plots of the films demonstrate a depressed semi-circular arc. The semicircle represents the parallel combination of bulk capacitance (because of immobile polymer

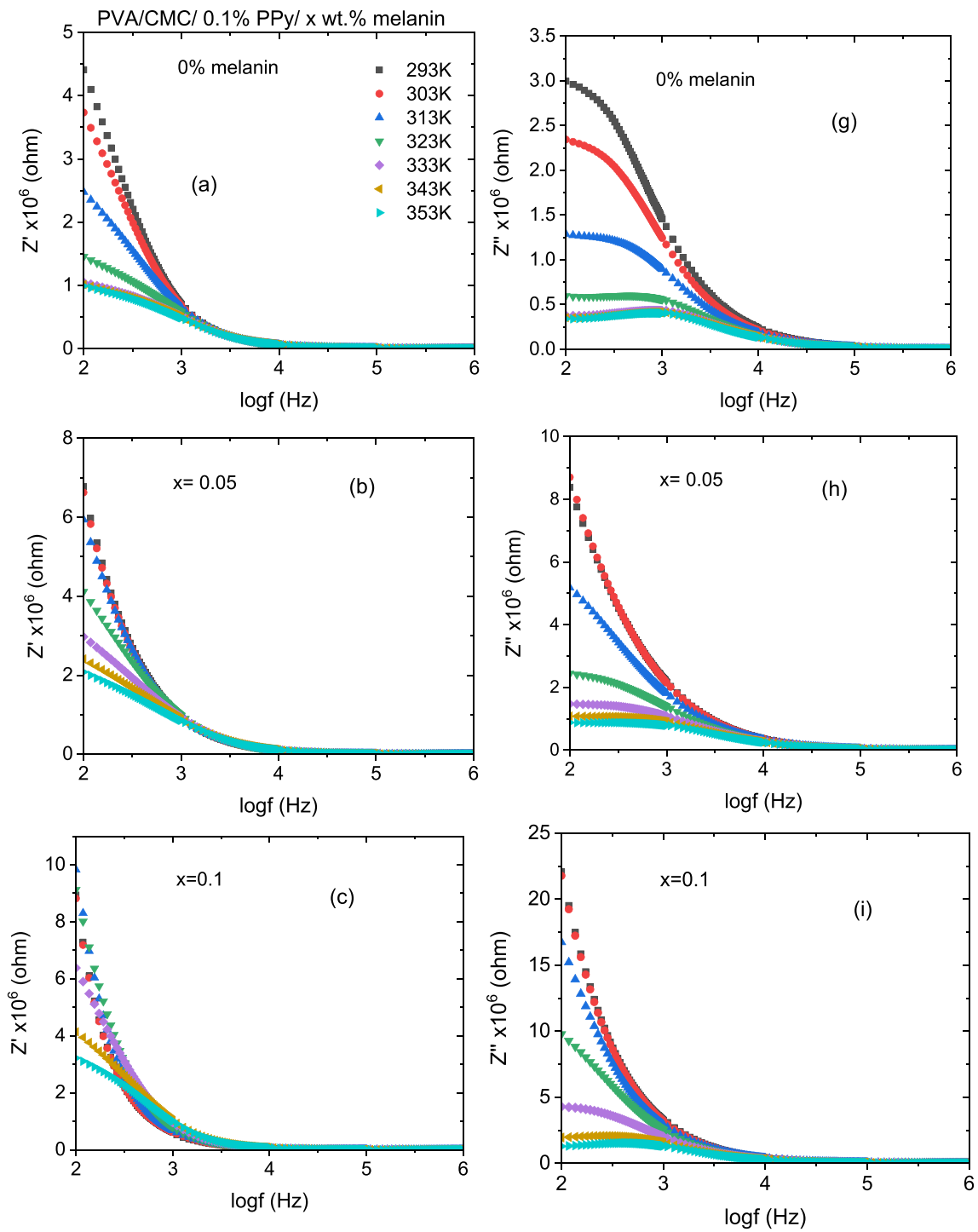


Fig. 12 Frequency dependence of the **a–f** real and **g–i** imaginary parts of complex impedance for PVA/CMC/PPy/x wt% Melanin blended polymers at different temperatures

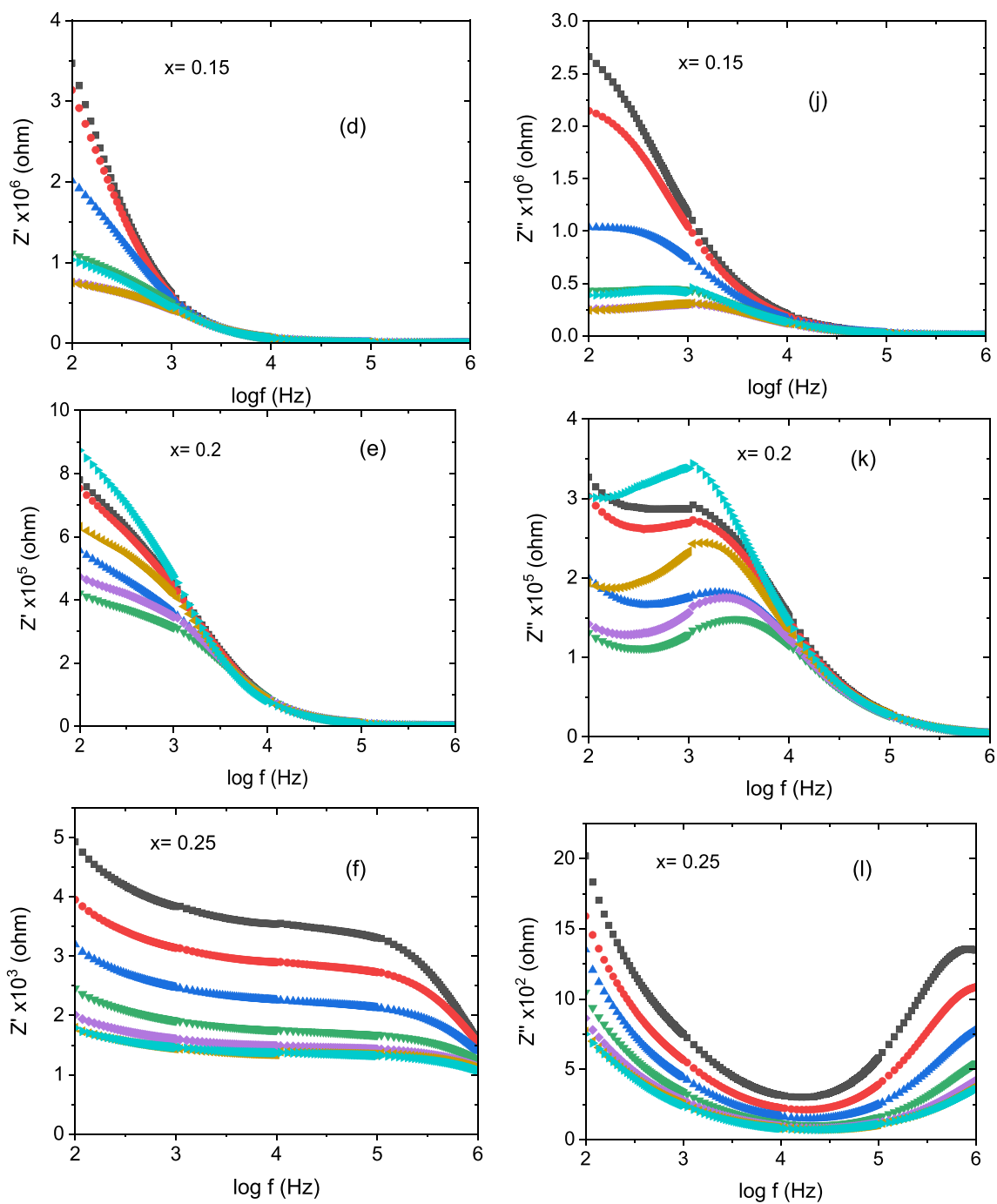


Fig. 12 (continued)

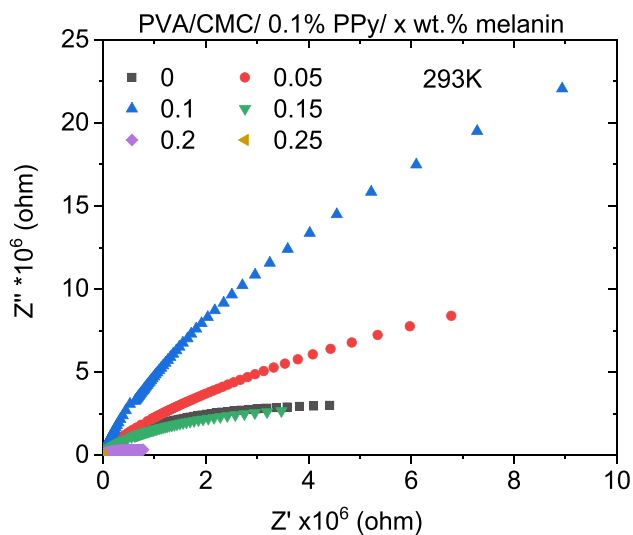


Fig. 13 Relation between Z' and Z'' for PVA/CMC/PPy/x wt% Melanin blended polymers at 293 K

chains) and bulk resistance (triggered by ion movement). The radius of each arc is affected by the quantity of melanin doping, which increases until $x=0.1$, then decreases with further melanin doping. This demonstrated that the conductivity of the doped blend rose as the quantity of melanin doping exceeded $x=0.1$ in the host blend. As the temperature rose in the doped blends the radius of the semicircular arc declined, i.e. the conductivity enhanced except in the blend with $x=0.2$, the radius of the semicircular arc changed with temperature irregularly, Fig. 14. This indicates the presence of an activated conduction mechanism [39]. Furthermore, a blend with $x=0.25$ has the inclined spike and the semicircle. The combination of an inclined spike and a semicircle represents the distinct conductive properties of ionic conducting materials [40]. The inclined spike indicates the formation of double layer capacitance at the interface between the electrode and electrolyte, which is caused by the movement of ions at low frequencies [41–43].

The real and imaginary components of the electric modulus (M' and M'') contribute significantly to the comprehension of the microscopic mechanisms underlying the material's relaxation and polarization processes. Figures 15a and b show the frequency dependence of M' and M'' for PVA/CMC/PPy/x weight percent melanin blended polymers at 293 K, respectively. At lower frequencies, the mobility of the charge carriers decreases due to the absence of the restoring force that governs it. As a result, the values of M' dropped but they reached zero in the blends with $x=0.2$ and 0.25 wt%. In the low-frequency region, M' values are low, indicating minimal electrode polarization. As the frequency rises, the M' value grows gradually in all blends. This effect, which is caused by the bulk impact, is a sign of the material's energy storage capability [44]. Depending on the quantity of melanin, the blends' M'' spectra demonstrate distinct relaxation peaks (one/two). The relaxation dynamics of the mobile ions are responsible for the emergence of these peaks [45].

The locations of the relaxation peaks were affected by the concentration of melanin, as shown in Fig. 15b. The observed shift may indicate a modification in the strength of the polymer chains, and hence modified the mobility of chain segments in the blends. The peak's amplitude decreases in the filled films compared to the pure blend, suggesting that melanin is involved in the relaxation process. Moreover, the asymmetry of the curve and the wide peaks in the M'' can be explained by the distribution of relaxation time and deviation from the ideal Debye behavior [46]. Analogous feature was observed in chemically synthesized conducting polyindole [47]. Figure 16 illustrates the temperature-dependent frequency variations of M' and M'' for each blend. As the temperature rises, the peaks progressively shift towards the higher frequency range. The displacement of peaks in response to increasing temperatures could potentially be attributed to the thermal generation of additional charge carriers.

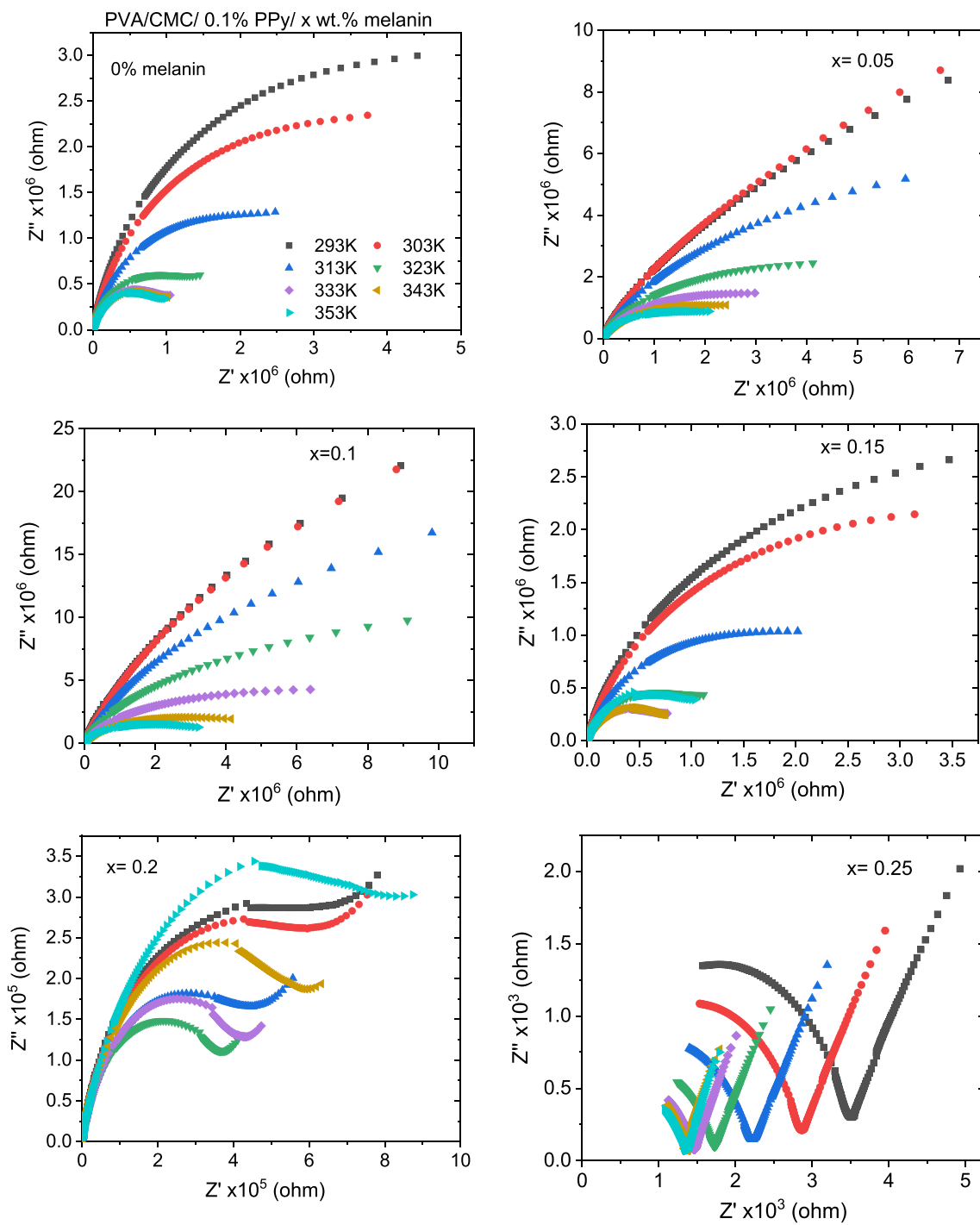


Fig. 14 Relation between Z' and Z'' for PVA/CMC/PPy/x wt% Melanin blended polymers at different temperatures

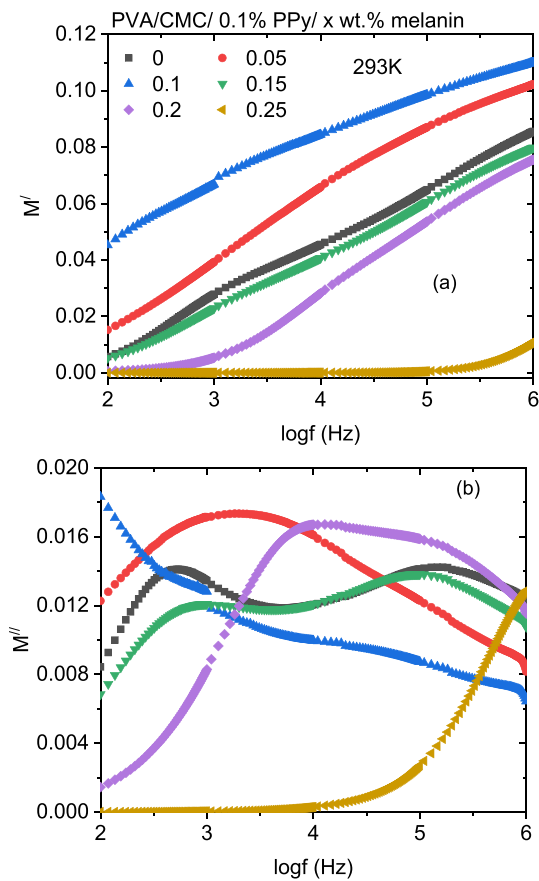


Fig. 15 Frequency dependence of the **a** real and **b** imaginary parts of electric modulus for PVA/CMC/PPy/x wt% Melanin blended polymers at 293 K

3.3 DC Conductivity Investigations

The temperature-direct current conductivity (σ_{dc}) relationship for PVA/CMC/PPy/x wt% melanin blended polymers is shown in Fig. 17. As the temperature rises, the σ_{dc} shows increasing values until it reaches its peak and then begins to decline. Depending on the temperature, the doped samples show either higher or lower dc conductivities than the undoped blend. Blend with $x=0.2$ has the highest dc conductivity. The degree of polymerization in doped blends affects the number of charge carriers that

spread out, which could explain the variance in σ_{dc} values of different blends [48]. The relationship between σ_{dc} and temperature in our blends resembles the characteristics of semiconductor materials. As shown by the following Arrhenius relation [49], the relationship between T and the change in σ_{dc} can be expressed:

$$\sigma = \sigma_o e^{\frac{-E_a}{k_B T}} \quad (10)$$

This formula can be rewrite as:

$$\ln \sigma = \ln \sigma_o - \frac{E_a}{k_B T} \quad (11)$$

where σ_o is a pre-exponential factor depending on the material, E_a is activation energy, T the absolute temperature and k_B is Boltzmann's constant. The activation energy (E_a) values for each sample are determined by computing the slope of the $\ln \sigma_{dc}$ versus $1000/T$ plots, as shown in Fig. 18. The undoped blend range exhibits two activation energy (E_a) values, specifically 0.06 eV and 0.53 eV, based on the temperature range. The E_a values of the host blend vary according to the level of melanin doping. The degree of melanin dispersion in the PVA/CMC/PPy matrix has an impact on the formation of conducting paths, which subsequently influences the conductivity and E_a values [50].

4 Conclusions

All blends have a semi-crystalline nature. The doped blends with melanin exhibit an increase in the level of roughness. As the percentage of melanin rose up to 0.1 wt%, the dielectric properties of the doped blend initially decreased, but subsequently rose again with further melanin doping. The dielectric constants of all the blends consistently increase as the temperature rises. The majority of PVA/CMC/PPy/x wt% melanin blended polymers can be considered suitable materials for energy storage. The σ_{ac} initially dropped when PVA/CMC/PPy was doped with melanin up to a concentration of 0.1 wt% but it gradually rose as the quantity of melanin was

further raised. The AC conductivity was enhanced as the temperature increased. Undoped and doped blends with melanin x up to 0.1 wt% follow the CBH model while the other doped blends follow the OLPT model. The electric impedance values of PVA/CMC/PPy/ x wt% melanin were grown by increasing the doping up to $x = 0.1$ wt% then

declined with increasing the quantity of dopant further. Blends with $x = 0.15$ and 0.2 wt% showed one relaxation peak, while doped blends with $x = 0.25$ wt% had two relaxation peaks. The relaxation time varies among the blends. The conductivity of the doped blend rose as the quantity of melanin doping exceeded $x = 0.1$ wt%. As

Fig. 16 Frequency dependence of the **a–f** real and **g–i** imaginary parts of electric modulus for PVA/CMC/PPy/ x wt% Melanin blended polymers at different temperatures

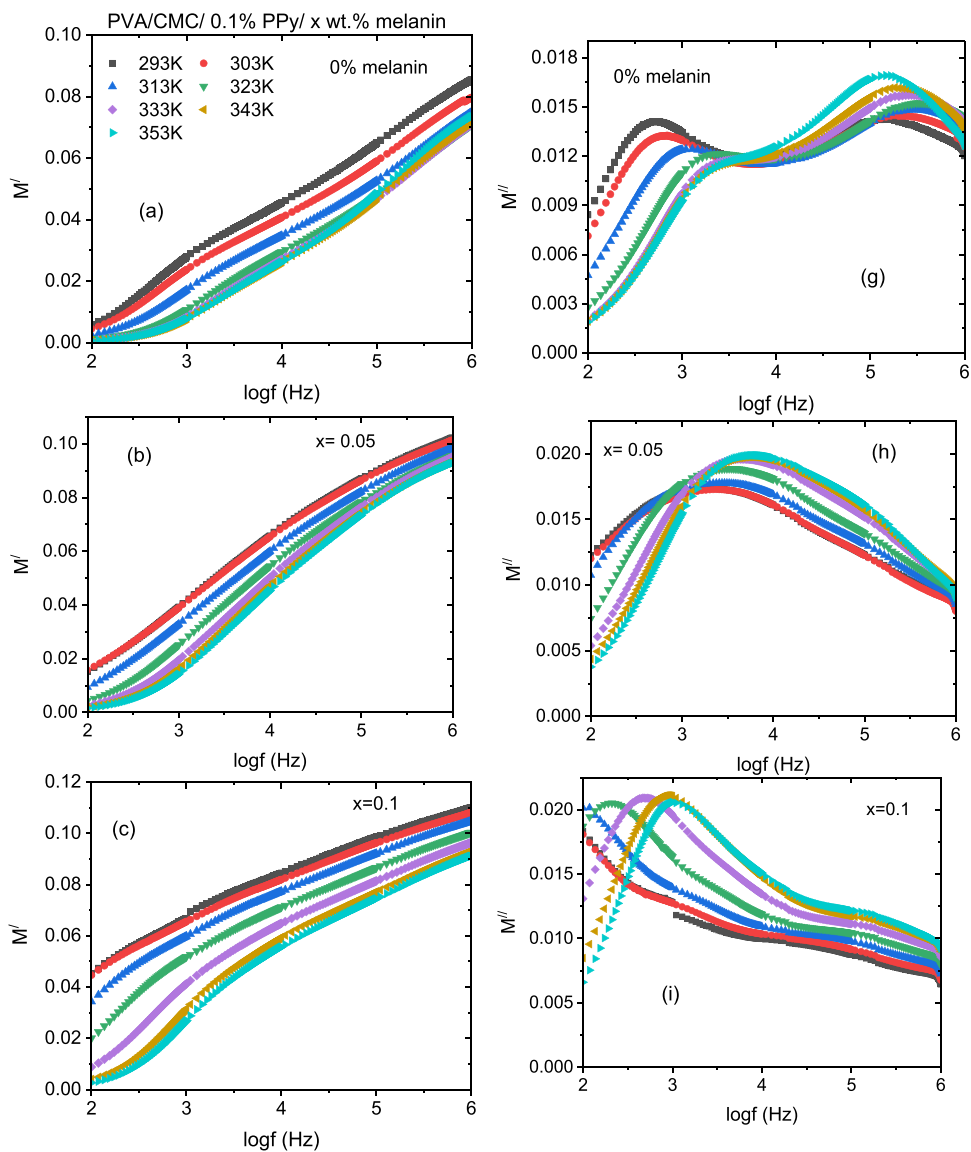
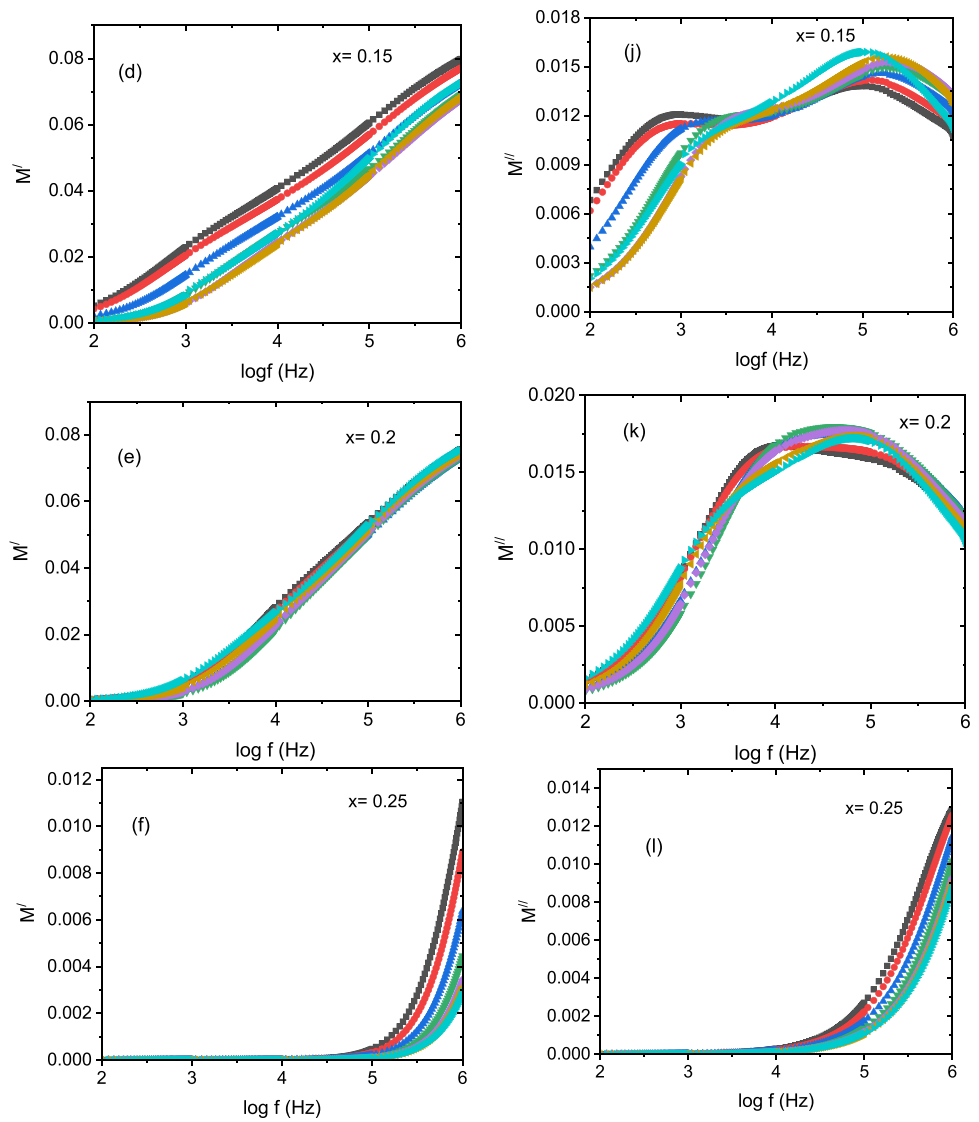


Fig. 16 (continued)



the temperature rose, the conductivity enhanced, except for the blend with $x = 0.2$ wt%, where the conductivity changed irregularly with temperature. The doped blend with $x = 0.25$ wt% has an inclined spike and a semicircle. Melanin is involved in the relaxation process. Depending on the quantity of melanin, the blends' M'' spectra demonstrate distinct relaxation peaks (one/two). Melanin is involved in the relaxation process. Depending on the temperature, the doped samples show either higher or lower dc conductivities than the undoped blend. The E_a values of the host blend vary according to the level of melanin doping.

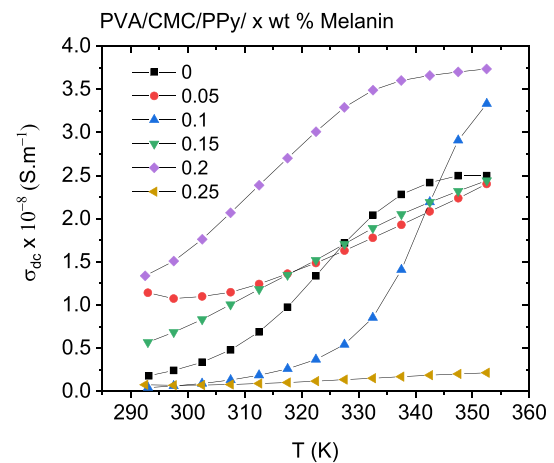


Fig. 17 Temperature dependence of dc conductivity for PVA/CMC/PPy/ x wt% Melanin blended polymers

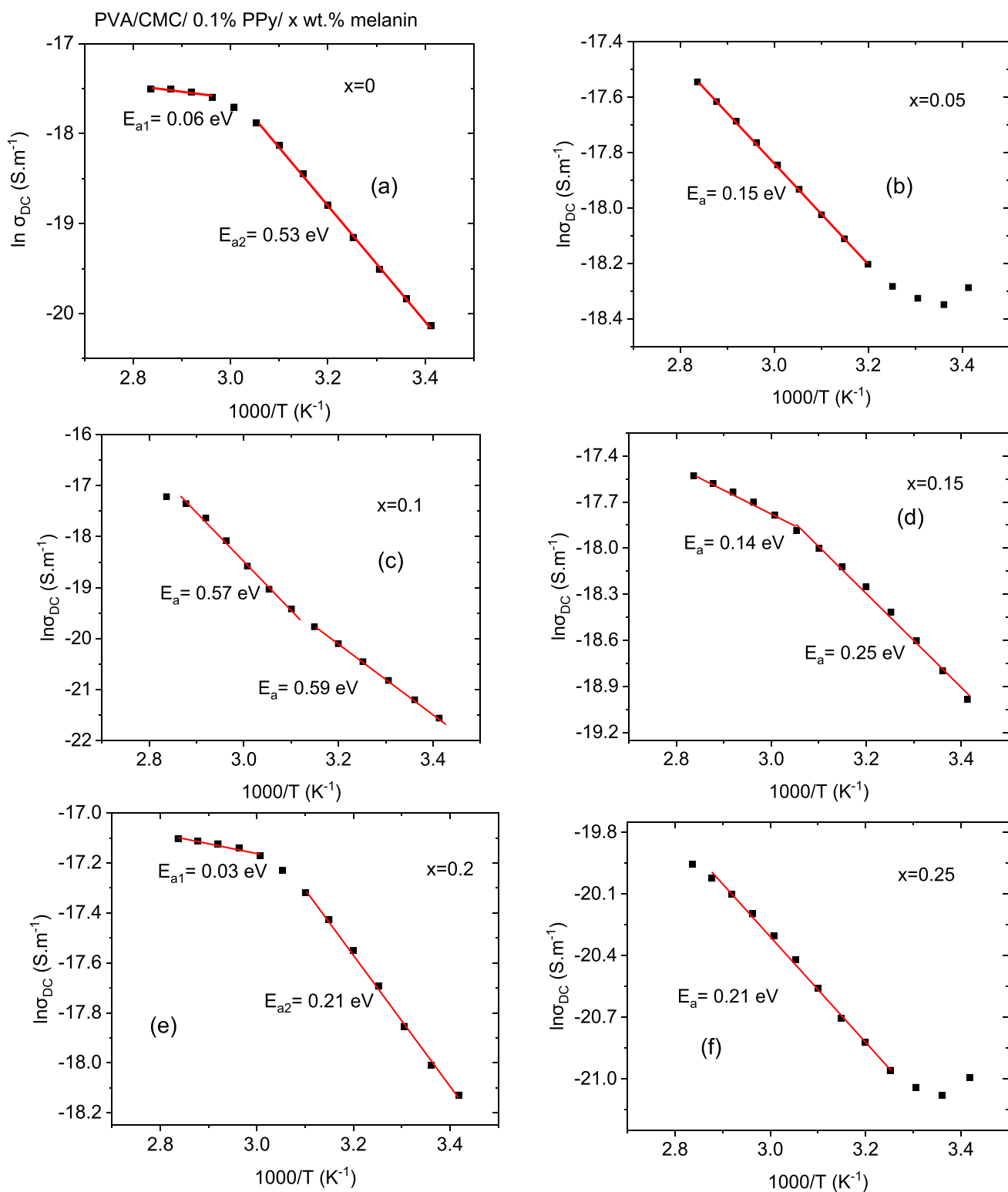


Fig. 18 a–f Relation between $\ln \sigma_{dc}$ and $1000/T$ for PVA/CMC/PPy/x wt% Melanin blended polymers

Author Contributions All authors have contributed, discussed the results and approved the final manuscript.

Funding This work is supported by Deanship of Scientific Research, King Saud University for funding through Vice Deanship of Scientific Research Chairs.

Data Availability The authors confirm that the data supporting the findings of this study are available within the article.

Declarations

Competing Interests The authors declare that they have no conflict of interest.

Ethical Approval We agreed all terms and conditions for Ethics approval.

References

1. A.M. El-naggar, Z.K. Heiba, A.M. Kamal, G. Lakshminarayana, M.B. Mohamed, Fabrication and adapting the optical, and dielectric performance of PVC/MnFe₂O₄/ZnMn₂O₄ nanocomposite films for optoelectronic applications. *Opt. Mater.* **152**, 115455 (2024)
2. Z.K. Heiba, A.M. El-naggar, A.M. Kamal, A.M. Aldhafiri, M.B. Mohamed, Influence of polyaniline on the structural, linear/non-linear optical, and dielectric characteristics of poly (vinyl chloride/poly (ethylene oxide) blends. *J. Macromol. Sci. Part B* **63**(5), 343 (2024)
3. P. Basu, A. Repanas, A. Chatterjee, B. Glasmacher, U.N. Kumar, I. Manjubala, PEO-CMC blend nanofibers fabrication by electrospinning for soft tissue engineering applications. *Mater. Lett.* **195**, 10 (2017)
4. S.F. Ng, N. Jumaat, Carboxymethyl cellulose wafers containing antimicrobials: a modern drug delivery system for wound infections. *Eur. J. Pharm. Sci.* **51**, 173 (2014)
5. P. Jayamurugan, V. Ponnuswamy, S. Ashokan, R.N. Jayaprakash, N. Ashok, K. Guna, R. Mariappan, DBSA doped polypyrrole blended with poly(4-styrenesulfonic acid) by mechanical mixing. *Mater. Sci.-Pol.* **32**, 648 (2014)
6. A.M. El-Naggar, Z.K. Heiba, A.M. Kamal, K.E. Alzahrani, O.H. Abd-Elkader, M.B. Mohamed, Impact of natural melanin doping on the structural, optical and dielectric characteristics of the PVP/CMC blend. *J. Taibah Univ. Sci.* **17**(1), 2190731 (2023)
7. K. Abdali, Structural, morphological, and gamma ray shielding (GRS) characterization of HVCMC/PVP/PEG polymer blend encapsulated with silicon dioxide nanoparticles. *SILICON* **14**, 9111 (2022)
8. S.A. Jabbar, S.M. Khalil, A.R. Abdulridha, E. Al-Bermany, A. Karar, Dielectric, AC conductivity and optical characterizations of (PVA-PEG) doped SrO hybrid nanocomposites. *Key Eng. Mater.* **936**, 83 (2022)
9. X. Lin, M. Wang, J. Zhao, X. Wu, J. Xie, J. Yang, Super-tough and self-healable all-cellulose-based electrolyte for fast degradable quasi-solid-state supercapacitor. *Carbohydr. Polym.* **304**, 120502 (2023)
10. K. Abdali, Structural, optical, electrical properties, and relative humidity sensor application of PVA/Dextrin polymeric blend loaded with silicon dioxide nanoparticles. *Mater Sci: Mater Electron* **33**, 18199 (2022)
11. N.S. Wadatkar, S.A. Waghuley, Enhancement in the optical and carbon dioxide gas sensing properties of polythiophene by dispersion of manganese dioxide nanoparticles. *Sustain. Chem. Clim. Act.* **4**, 100036 (2024)
12. S.A. S-Mirmahalleh, S.N. Eliseeva, A.R. Moghaddam, H. R-Mamaqani, M. S-Kalajahi, Synthesis and evaluation of cellulose/polypyrrole composites as polymer electrolytes for lithium-ion battery application. *Int. J. Biol. Macromol.* **262**, 129861 (2024)
13. X. Pan, M. Wang, X.G. Qi, N. Zhang, T. Huang, J. Yang, Y. Wang, Fabrication of sandwich-structured PPy/MoS₂/PPy nanosheets for polymer composites with high dielectric constant, low loss and high breakdown strength. *Composites Part A: Appl. Sci. Manuf.* **137**, 106032 (2020)
14. L. Yang, F. Lin, F. Zabihi, S. Yang, M. Zhu, High specific capacitance cotton fiber electrode enhanced with PPy and MXene by in situ hybrid polymerization. *Int. J. Biol. Macromol.* **181**, 1063 (2021)
15. L.M. Swain, S. Acharya, B.P. Sahoo, Dielectric properties of polypyrrole and polyvinylidene fluoride blends: effect of temperature. *Mater. Today: Proc.* (2023). <https://doi.org/10.1016/j.matpr.2023.12.036>
16. F.H. Alkallas, S.M. Alghamdi, O. Albeydani, E.A. Rashed, E. Alsubhe, A. Ben, G. Trabelsi, E.A. Mwafy, W.B. Elsharkawy, A.M. Mostafa, Studying the effect of addition of lithium titanate on crystallinity and electrical properties of PPy-C/PVA nanocomposites for optoelectronic applications. *J. Mater. Res. Technol.* **28**, 3414 (2024)
17. S. Jha, D. Tripathi, Dielectric and electrical study of PPy doped PVA-PVP films. *AIP Conf. Proc.* **1953**, 050073 (2018)
18. N. Al-Shamery, T. Benselfelt, P.S. Lee, Melanin and polypyrrole-coated nanocellulose hydrogel networks for environmental sensing and energy storage. *ACS Appl. Mater. Interfaces* **15**(21), 25966 (2023)
19. N.L. Nozella, J.V. Lima, R.F. de Oliveira, G.C.F. de Oliveira, Melanin/PEDOT:PSS blend as organic mixed ionic electronic conductor (OMIEC) for sustainable electronics. *Mater. Adv.* **4**, 4732 (2023)
20. L. Agrawal, S.K. Vimal, P. Barzaghi, T. Shiga, M. Terenzio, Biodegradable and electrically conductive melanin-poly (3-hydroxybutyrate) 3D fibrous scaffolds for neural tissue engineering applications. *Macromol. Biosci.* **22**, 2200315 (2022)
21. M. Das, D. Sarkar, Development of room temperature ethanol sensor from polypyrrole (PPy) embedded in polyvinyl alcohol (PVA) matrix. *Polym. Bull.* **75**, 3109 (2018)
22. C.M. Tang, Y.H. Tian, S.H. Hsu, Poly(vinyl alcohol) nanocomposites reinforced with bamboo charcoal nanoparticles: mineralization behavior and characterization. *Materials* **8**, 4895 (2015)
23. R. Megha, Y.T. Ravikiran, S. Kotresh, S.C. Vijaya Kumari, H.G.R. Prakash, S. Thomas, Carboxymethyl cellulose: an efficient material in enhancing alternating current conductivity of HCl doped polyaniline. *Cellulose* **25**, 1147 (2018)
24. X. Chen, J.-K. Tseng, I. Treufeld, M. Mackey, D.E. Schuele, R. Li, M. Fukuto, E. Baer, L. Zhu, Enhanced dielectric properties due to space charge-induced interfacial polarization in multilayer polymer films. *J. Mater. Chem. C* **5**, 10417 (2017)
25. M. Morsi, A. Rajeh, A. Al-Muntaser, Reinforcement of the optical, thermal and electrical properties of PEO based on MWCNTs/Au hybrid fillers: Nanodielectric materials for organoelectronic devices. *Compos. B Eng.* **173**, 106957 (2019)
26. E.A. Rabiea, A.S. Abouhaswa, H.M. Abomostafa, Structural, dielectric, and optical properties based on spinel ferrite (Mn_{0.5}Fe_{1.5}Mg_{0.5}Ni_{0.5}O₄) nanoparticles filler reinforced PVA for optoelectronic, laser CUT-OFF filters and energy storage devices. *J. Phys. D Appl. Phys.* **57**, 035301 (2024)
27. I. Yahia, N. Hegab, A. Shakra, A. Al-Ribaty, Conduction mechanism and the dielectric relaxation process of a-Se75Te25-xGax

- ($x=0, 5, 10$ and 15 at wt%) chalcogenide glasses. *Phys. B* **407**, 2476 (2012)
28. A. Awadhia, S.K. Patel, S.L. Agarwal, Dielectric investigations in PVA based gel electrolytes. *Prog. Cryst. Growth Charact. Mater.* **52**, 61 (2006)
 29. N.S. Wadatar, S.A. Waghuley, Studies on properties of as-synthesized conducting polythiophene through aqueous chemical route. *J. Mater. Sci. Mater. Electron.* **27**, 10573 (2016)
 30. N.F. Mott, E.A. Davis, *Electronic processes in non-crystalline materials (Monographs on Physics)* (Oxford University Press, Oxford, 1979)
 31. K. Hemalatha, G. Sriprakash, M. Ambika Prasad, R. Damle, K. Rukmani, Temperature dependent dielectric and conductivity studies of polyvinyl alcohol-ZnO nanocomposite films by impedance spectroscopy. *J. Appl. Phys.* **118**, 154103 (2015)
 32. A.K. Jonscher, The universal dielectric response. *Nature* **267**, 673 (1977)
 33. M. Sassi, A. Bettaibi, A. Oueslati, K. Khirouni, M. Gargouri, Electrical conduction mechanism and transport properties of LiCrP2O7 compound. *J. Alloy. Compd.* **649**, 642 (2015)
 34. T. Rhimi, M. Toumi, K. Khirouni, S. Guerhazi, AC conductivity, electric modulus analysis of KLi(H₂PO₄)₂ compound. *J. Alloys Compd.* **714**, 546 (2017)
 35. S. Selvasekarapandian, M. Vijayakumar, The ac impedance spectroscopy studies on LiDyO₂. *Mater. Chem. Phys.* **80**, 29 (2003)
 36. A.R. James, K. Srinivas, Low temperature fabrication and impedance spectroscopy of PMN-PT ceramics. *Mater. Res. Bull.* **34**, 1301 (1999)
 37. M. Ram, Synthesis and electrical properties of (LiCo₃/5Fe₁/5Mn₁/5) VO₄ ceramics. *Solid State Sci.* **12**, 350 (2010)
 38. K. Chandra, K. Prasad, R. Gupta, Impedance spectroscopy study of an organic semiconductor: Alizarin. *Physica B* **388**, 118 (2007)
 39. M. Abbassi, R. Ternane, I. Sobrados, A. Madani, M. Trabelsi-Ayadi, J. Sanz, *Ceram. Int.* **39**, 9215 (2013)
 40. M. Prabu, S. Selvasekarapandian, A. Kulkarni, G. Hirankumar, A. Sakunthala, Ionic conductivity studies on LiSmO₂ by impedance spectroscopy. *Ionicity* **16**, 317 (2010)
 41. O. Bohnke, S. Ronchetti, D. Mazza, Conductivity measurements on nasicon and Nasicon-modified materials. *Solid State Ion.* **122**, 127 (1999)
 42. X. Li, S. Hsu, An analysis of the crystallization behavior of poly(ethylene oxide)/poly(methyl methacrylate) blends by spectroscopic and calorimetric techniques. *J. Polym. Sci. Polym. Phys. Ed.* **22**, 1331 (1984)
 43. C. Ramya, S. Selvasekarapandian, G. Hirankumar, T. Savitha, P. Angelo, Investigation on dielectric relaxations of PVP-NH₄SCN polymer electrolyte. *J. Non-Cryst. Solids* **354**, 1494 (2008)
 44. C. Chen, A. Kine, R.D. Nelson, J.C. LaRue, Impedance spectroscopy study of conducting polymer blends of PEDOT: PSS and PVA. *Synth. Met.* **206**, 106 (2015)
 45. N. Gondaliya, D. Kanchan, P. Sharma, P. Joge, Effect of silicone dioxide and poly (ethylene glycol) on the conductivity and relaxation dynamics of poly (ethylene oxide)-silver triflate solid polymer electrolyte. *J. Appl. Polym. Sci.* **125**, 1513 (2012)
 46. S. Nath, S.K. Barik, S. Hajra, R. Choudhary, Relaxation mechanism, conductivity and multiferroic property studies in (La₁/2Li₁/2)(Fe₂/3W₁/3) O₃. *Phys. B* **567**, 100 (2019)
 47. N.S. Wadatar, S.A. Waghuley, A novel studies on electrical behaviour of chemically synthesized conducting polyindole. *Indian J. Phys.* **92**(12), 1551 (2018)
 48. N.S. Wadatar, S.A. Waghuley, Characterizing the electro-optical properties of polyaniline/poly(vinyl acetate) composite films as-synthesized through chemical route. *Res Surf Interfaces.* **4**, 100016 (2021)
 49. G.M. Asnag, A.H. Oraby, A.M. Abdelghany, Green synthesis of gold nanoparticles and its effect on the optical, thermal and electrical properties of carboxymethyl cellulose. *Compos. B* **172**, 436 (2019)
 50. A.M. El Sayed, S. Saber, Structural, optical analysis, and Poole-Frenkel emission in NiO/CMC-PVP: Bio-nanocomposites for optoelectronic applications. *J. Phys. Chem. Solids* **163**, 110590 (2022)

Publisher's Note Springer Nature remains neutral with regard to jurisdictional claims in published maps and institutional affiliations.

Springer Nature or its licensor (e.g. a society or other partner) holds exclusive rights to this article under a publishing agreement with the author(s) or other rightsholder(s); author self-archiving of the accepted manuscript version of this article is solely governed by the terms of such publishing agreement and applicable law.